Clinical & Experimental Metastasis
https://doi.org/10.1007/s10585-018-9923-9

REVIEW

Frontiers of cancer imaging and guided therapy using ultrasound, light, and microwaves

Russell S. Witte[1] · Chandra Karunakaran[1] · Andres N. Zuniga[1] · Hannah Schmitz[1] · Hina Arif[1]

Received: 2 July 2018 / Accepted: 5 July 2018

Abstract

This review describes emerging techniques within the last 5 years that employ ultrasound for detecting and staging malignancy, tracking metastasis, and guiding treatment. Ultrasound elastography quantifies soft tissue elastic properties that change as a tumor grows and proliferates. Hybrid imaging modalities that combine ultrasound with light or microwave energy provide novel contrast for mapping blood oxygen saturation, transport of particles through lymphatic vessels and nodes, and real-time feedback for guiding needle biopsies. Combining these methods with smart nanoparticles and contrast agents further promotes new paradigms for cancer imaging and therapy.

Keywords Photoacoustic imaging · Thermoacoustic imaging · Ultrasound Elastography · Shear wave imaging · Image-guided therapy · Personalized medicine

This review describes emerging techniques within the last 5 years that employ ultrasound for detecting and staging malignancy, tracking metastasis, and guiding treatment. Ultrasound elastography quantifies soft tissue elastic properties that change as a tumor grows and proliferates. Hybrid imaging modalities that combine ultrasound with light or microwave energy provide novel contrast for mapping blood oxygen saturation, transport of particles through lymphatic vessels and nodes, and real-time feedback for guiding needle biopsies. Combining these methods with smart nanoparticles and contrast agents further promotes new paradigms for cancer imaging and therapy.

Presented at the 7th International Cancer Metastasis Symposium in San Francisco, CA from April 20–22, 2017 (www.cancermetastasis.org).

✉ Russell S. Witte
rwitte@radiology.arizona.edu

[1] Department of Radiology, University of Arizona, Tucson, AZ 85724, USA

Ultrasound elasticity and shear wave imaging

Two elastographic techniques have emerged over the past several years for detecting cancer, classifying suspicious lesions, reducing false positives, and guiding biopsies. Quasi-static transient elastography quantifies displacement and strain as tissue deforms to identify relative regions of soft and hard tissue. Traditional elastography for diagnostic breast imaging revealed strain patterns remarkably different for benign and malignant masses during a multicenter clinical trial [1]. Unlike benign fibroadenomas, malignant tumors like ductal carcinomas typically integrate with surrounding tissue such that the resulting strain map reveals stiff boundaries in a predictable pattern that extend beyond the margins of the lesion defined by B mode ultrasound. A more recent study indicated that *nonlinear* elastic properties can further improve classification of suspicious lesions [2]. 3D ultrasound was integrated into a conventional mammography system to track deformation over the full range of compression. By rotating a linear US array near the region of interest, 3D B mode and strain maps were acquired, facilitating volumetric segmentation of the lesions and quantifying a nonlinear elastic parameter. Not only were malignant tumors stiffer than benign lesions ($p < 0.05$), they also exhibited load-dependent elastic properties with a stiffness directly proportional to the

Published online: 04 August 2018

applied compressive force ($p < 0.001$). It may be possible, therefore, to integrate 3D US into mammography to track nonlinear elastic properties for better classification of suspicious lesions and reduce false positive biopsies.

Ultrasound shear wave imaging (USWI) is another method growing in popularity that quantifies the elastic shear modulus near a region of interest. In USWI, a radiation force "push" pulse generates shear waves that propagate perpendicular to the US beam away from the focus. A fast sequence of plane waves is then used to track tissue displacement and determine the shear wave velocity ν such that the shear modulus is directly proportional to ν^2. Most modern clinical US systems now feature USWI, including the Aixplorer by SuperSonic Imagine, Acuson S3000 by Siemens Medical Solutions, and most recently the T-SWE by Toshiba Medical System. A recent study tested the T-SWE system for detecting breast lesions and evaluated its diagnostic performance in 218 patients [3]. Receiver operating characteristic (ROC) analysis identified both quantitative and qualitative factors that substantially improved diagnostic performance for differentiating breast lesions. A cut-off value of 36.1 KPa for the elastic modulus yielded sensitive (85.1%), specific (96.6%) and accurate (94.2%) results with an area under the curve (AUC) of 0.943. Qualitative color patterns further revealed much greater heterogeneity for malignant tissue with a positive predictive value (PPV) of 87.0%, and negative predictive value (NPV) of 96.1%. While these results need to be confirmed at other sites in a larger patient population, this study illustrates the potential of USWI as a non-invasive method for classifying breast lesions.

Identification of malignant cervical lymph nodes (LN) is critical due to a nearly 50% risk of distant mestastases in individuals who have more than three histologically positive LNs versus individuals without nodal metastasis [4]. Additionally, individuals who are diagnosed with nasopharyngeal carcinoma (NPC) have about 85% chance of developing cervical LN metastasis [5]. Due to the small size of lymph nodes, USWI has an advantage over conventional MRI with regards to non-invasive characterization and determination of malignancy. In a 2016 study, researchers studied cervical LNs on the ACUSON S3000 and determined from ROC analysis that there were 2 critical cutoff values [6]. First, a shear wave velocity of 2.93 m/s produced a sensitivity of 92.59%, specificity of 75.46%, PPV of 48.54%, and NPV of 97.6%; a second, cutoff at 3.2 m/s offered a sensitivity of 79.63%, specificity of 81.94%, PPV of 52.44%, and NPV of 94.15%. A more recent study further assessed cervical LN malignancy using USWI on the Aixplorer and reported sensitivity (84.6%), specificity (83.1%), accuracy (83.3%), PPV (59.5%), and NPV (94.8%) for detected cancer [7]. Currently, USWI is quite effective as a negative predictor for the presence of a tumor, but there is room for improvement as a positive predictor of cervical LNs as standardized methods are being developed across platforms and industry [8].

USWI is also being used to evaluate thyroid nodules, which are very common and rising in incidence with increasing age, those with iodine deficiency, after exposure to radiation, and in the female population. Prevalence of thyroid nodules is reported as 2–6% with palpation on physical examination, 19–35% with ultrasound, and 8–65% in autopsy data. Following clinical examination, thyroid ultrasound is used as a first-line test to differentiate benign and malignant nodules. While high-resolution US is excellent for detecting thyroid lesions, it has suboptimal accuracy for predicting malignancy based on grayscale and Doppler sonographic criteria, which typically includes hypoechogenicity, microcalcifications, irregular margins, lobulated margins, perinodular thyroid parenchyma invasion, taller-than-wide shape and presence of vascularity. USWI, on the other hand, has merged as a promising tool for thyroid cancer detection because malignancies are usually stiffer than benign lesions. USWI can be helpful particularly in stratifying suspicious nodules in patients with multiple thyroid nodules. These nodules are either followed up on imaging or undergo fine needle aspiration for definitive tissue characterization. Azizi et al. identified a single cut-off of 3.54 m/s for the maximum shear wave velocity for predicting thyroid cancer and reported sensitivity, specificity , PPV and NPV values of 79.3, 71.5, 26.8 and 96.3%, respectively. In Fig. 1, two examples are presented captured on the ACUSON S3000 at Banner University Medical Center in Tucson, Arizona.

A new technique is also being developed on the Acuson S3000 that enables fusion of MRI with USWI and B mode ultrasound for feedback during prostate needle biopsies. Co-registration of these different modalities provide critical information for tracking the position and triggering the needle to biopsy the core as described in Fig. 2.

Photoacoustic imaging

Photoacoustic imaging (PAI) implements a short laser pulse to induce transient heating in tissue, thermoelastic expansion, and generation of ultrasonic waves. These waves are then detected by an array of ultrasound receivers to produce high contrast images two or more centimeters deep based on the absorption of the laser pulse. In recent years, commercial platforms with wavelength-tunable lasers have emerged to study the tumor microenvironment, improve the decision to biopsy, guide resection of the sentinel lymph node (SLN), and track transport through lymphatic vessels and nodes.

In 2015, Seno Medical Instruments completed Phase II clinical trials of its photoacoustic breast imaging system called the Imagio™. Sixteen centers participated in the prospective multicenter study, assessing 1808 breast masses

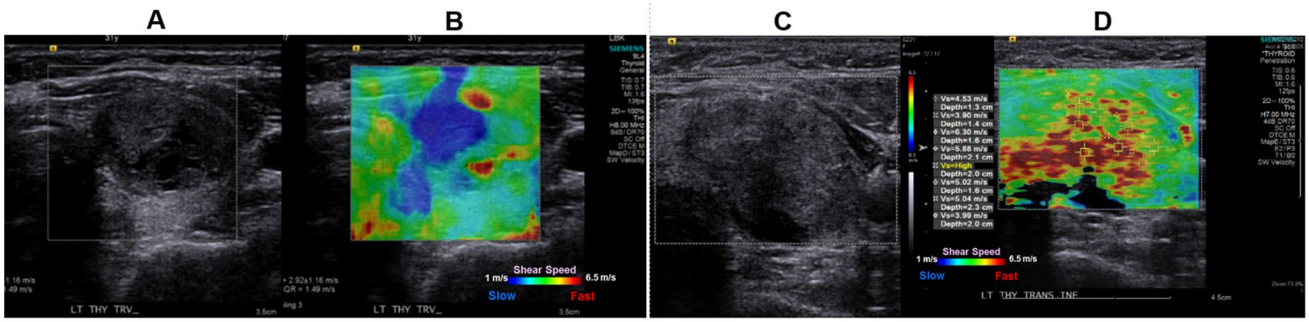

Fig. 1 (left) B mode (gray, **a**) and shear wave (color, **b**) images of a benign thyroid nodule in female of 31 years. Blue regions near nodule indicate slow shear wave velocities (~ 1 m/s) and softer tissue. (right) Heterogeneously hypoechoic solid left thyroid nodule without significant internal vascularity reveals non-specific features on B mode in female of 23 years (**c**). Red regions near center of lesions on USWI (**d**) denote fast shear velocities (> 6.5 m/s) and stiffer tissue, suggesting malignancy. Targeted biopsy of this nodule revealed papillary thyroid cancer. All images acquired on the Acuson S3000 [unpublished data]. (Color figure online)

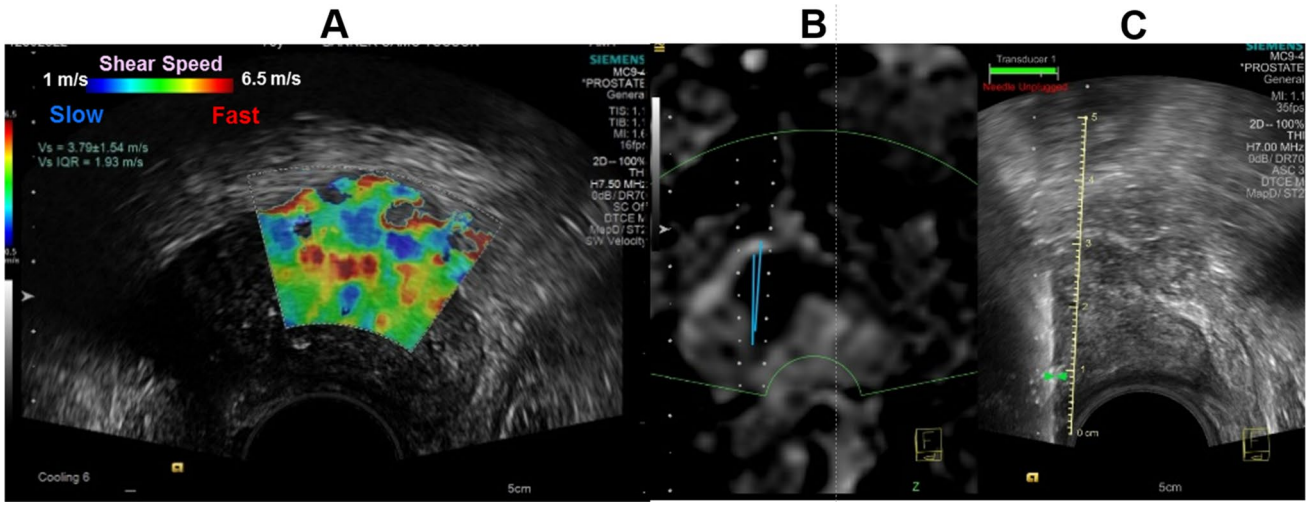

Fig. 2 72-year-old male with rising PSA levels. USWI through the anterior part of the gland indicates stiff region (red) suggestive of cancer (**a**). Multiparametric MR imaging confirmed presence of prostate adenocarcinoma (PIRADS-4). MR directed US guided fusion biopsy registration workflow is depicted with side-to-side MR and US images at corresponding axial level (**b**). Note the biopsy track on US has a corresponding identical track on apparent diffusion coefficient (ADC) image. Lesion is targeted on ultrasound with 18-gauge core biopsy needle within the dotted track on the shown-on sonogram using MR image as guide (**c**). Blue marker on MR image represents the acquired core in the PIRADS-4 Lesion. Green-bow at the proximal end on the needle track denotes the start point of the core, corresponding to the site of fire for the biopsy. Pathology revealed prostatic adenocarcinoma [unpublished data]. (Color figure online)

in 1739 subjects. The scoring system focused on vascularity and blood oxygen saturation in and around suspicious lesions (Fig. 3). Combined with B mode ultrasound, the PAI system was able to downgrade 40.8% of benign mass reads with 43.0% specificity compared to 28.1% specificity for ultrasound alone. The results suggest that with continued improvement in the scoring system, the hybrid imaging platform may help downgrade benign masses classified as Breast Imaging Reporting and Data System (BI-RADS) 4a and 4b to BI-RADS 3 or 2 [9].

In 2018, noting limitations in previous PA breast imaging systems, a research team at Caltech and Washington University developed and tested a cutting-edge—and potentially revolutionary—PA computed tomography (PACT) platform capable of 3D imaging of the human breast within a single-breath hold (SBH) [10]. The fully-tomographic PACT system achieved 3D isotropic spatial resolution of 0.25 mm (four times better than MRI) and deep penetration of 40 mm to map angiogenesis and blood oxygen saturation *without* contrast agents. Blood vessel density was used as the primary biomarker to identify eight of nine biopsied tumors in a pilot study of eight subjects (sensitivity/true positive of 88%, specificity/true negative of 80%, seven breast cancer patients, and one volunteer). Figure 4 presents sample

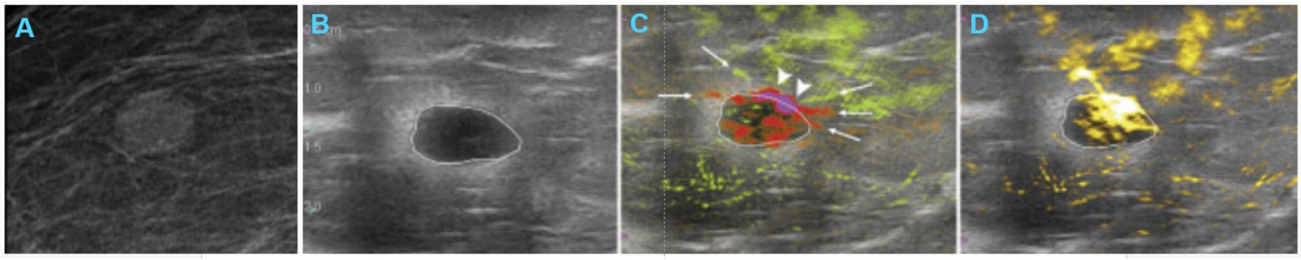

Fig. 3 Grade II invasive ductal carcinoma depicted on conventional mammography (**a**), ultrasound (**b**), and Imagio™ PAI platform (**c, d**). In **c**, deoxygenated vessels (red) appear inside lesion enclosed by white line. In **d**, total hemoglobin (yellow) was concentrated inside lesion. This mass was upgraded from BI-RADS 4a (at B mode US and Doppler) to BI-RADS 4c (Imagio™). Credit: Menezes et al., Radiological Society of North America [9]. (Color figure online)

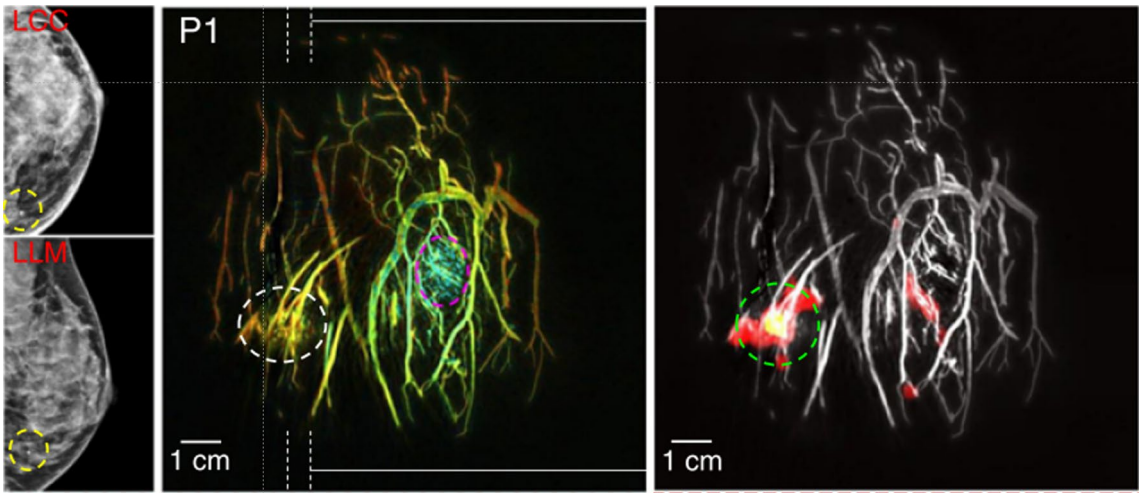

Fig. 4 (left) X-ray mammogram of a 48 year-old female with an invasive lobular carcinoma (grade 1/3) denoted by dashed ellipses. *LCC* left cranial caudal, *LLM* left lateral-medio; (middle) depth-encoded angiograms mapped by PACT system with single breath hold. (right) Automatic tumor detection was based on high blood vessel density maps (hot colors) superimposed on grayscale PACT image. Credit: Modified from Lin et al., Nature Publishing [10]. http://creativecommons.org/licenses/by/4.0/. (Color figure online)

images from a patient with invasive lobular carcinoma. As a safe, noninvasive, and high resolution imaging system, the PACT may emerge as a breakthrough technology for real-time volumetric diagnostic imaging of the breast with strong contrast for detecting and classifying tumors. Moreover, with endogenous contrast based on hemoglobin and blood oxygen saturation, clinical platforms for PA imaging may also help monitor response to neoadjuvant chemotherapy in real-time and with superior resolution than dynamic contrast-enhanced MRI.

Other PAI systems have been evaluated for noninvasive detection of the SLN. Standard methods require radiolabeled sulfur colloid and/or methylene blue dye to help identify the SLN and guide surgical resection. However, conventional methods are invasive leading to increased morbidity. Philips modified their iU22 clinical ultrasound scanner to produce a combined PAI and ultrasound platform for 3D noninvasive mapping of the SLN using Methylene Blue (MB), an FDA-approved dye that strongly absorbs light at long wavelengths (~670 nm) [11]. The dual-wavelength system was able to distinguish lymphatic vessels (LVs) and nodes, as well as blood vessels. Initial results suggest that integrating PAI and ultrasound during fine needle aspiration biopsies could eliminate the need for invasive axillary staging procedures. The approach can also be highly quantitative. One group recently described lymphatic pumping in mice using a state-of-the-art high resolution (<0.1 mm) PAI and ultrasound imaging system by Visualsonics (LAZR-X). Pumping of afferent LVs and filling of the perilymph and popliteal nodes were quantified in real-time using a 40 MHz ultrasound array following a subcutaneous injection of indocyanine green (ICG), a strong near-infrared absorber and PA contrast agent (Fig. 5) [12].

A recent clinical study of 506 SLNs in 214 melanoma patients on iThera's Multispectral Optoacoustic Tomography (MSOT) system further revealed that PAI is able to detect regional lymph node metastasis based on the intrinsic absorption of melanin [13]. While sensitivity for detecting

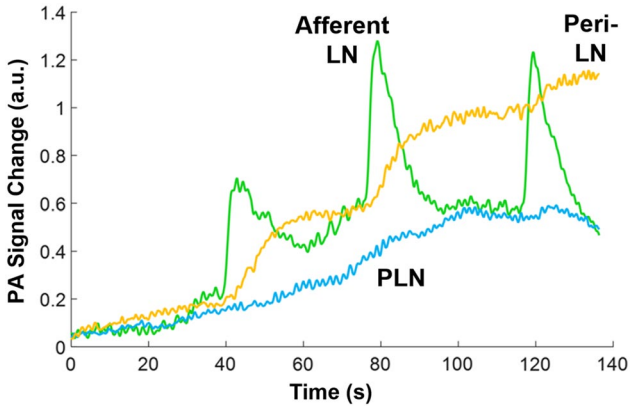

Fig. 5 Change in PA signal after subcutaneous injection of methylene blue. The popliteal node (PLN) is filling continuously during the 120 s, while the afferent lymph node (LN) exhibits pumping activity every 40 s. The Peri-LNs also fill periodically with the pumping of the afferent LN. Credit: Forbrich et al., SPIE Publication [12]

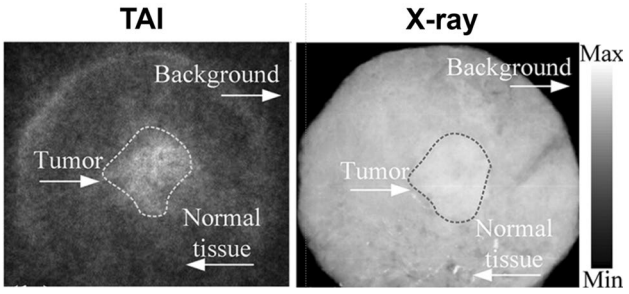

Fig. 6 (left) TA image of a human breast tumor embedded in an excised ewe breast using ultrashort microwave pulses and a 10 MHz full ring ultrasound array. (right) Corresponding X-ray image of the same sample. Dotted outline indicates the boundary of the tumor. Credit: Ye et al., IEEE Publishing [19]

metastasis was high, specificity (48.6%) was low. A study by Luke et al. demonstrated in mice that molecularly activated nanosensors as smart PA contrast agents might be a better option to improve specificity for detecting distant micrometastases [14]. Alternatively, phase-transition nanodroplets might be an ideal contrast agent for PA imaging and therapy. Yang et al., for example, incorporated strongly-absorbing carbon nanotubes (CNTs) into phase-transition nanodroplets to not only detect LNs with PAI, but, with increased incident laser energy, the nanoparticles were able to destroy breast cancer cells in vitro and in vivo due to a photothermal effect [15].

Thermoacoustic imaging

Microwave-induced thermoacoustic imaging (TAI) exploits the same physical principal as PAI, except that short electromagnetic pulses between 0.3 and 3 GHz are used as the source for excitation and images are proportional to the absorbed microwave energy. Because tumors with higher water content differentially absorb microwaves compared to surrounding tissue (e.g., adipose), TAI has been proposed as a novel approach for diagnostic breast imaging, and a pilot study at 434 MHz revealed 3D in vivo images of the human breast with excellent sensitivity for detecting tumors [16]. However, limitations in microwave and ultrasound hardware in these early studies prevented high resolution characterization and accurate classification of suspicious lesions. Because resolution in TAI depends on the duration of the excitation pulse, the long microwave pulse of 1 μs contributed to poor spatial resolution (> 1 mm). To overcome this drawback, two research teams recently tested a novel broadband transmitter for TAI with ultrashort impulse excitation [17, 18]. Instead of a traditional tube-based amplifier, the low-cost excitation source exploited a high-voltage triggered spark gap for generating short electromagnetic impulses (10 ns duration) with high peak power (up to 40 MW). One study evaluated the new transmitter and curved 7.5 MHz ultrasound array for imaging a tumor in an excised breast of a ewe and reported a resolution of less than 0.2 mm and a mean contrast-to-noise ratio of 2.8 compared to 1.7 with standard X-ray (Fig. 6) [19]. Moreover, the energy density for detection (21.8 μJ/cm^2) was much less than the safety threshold for microwave exposure.

Another recent study extended applications of TA technology from cancer imaging to therapy. Ultrashort microwave pulses were combined with superparamagnetic iron oxide nanoparticles (SPIO) functionalized with Human Serum Albumin (HSA-SPIO) as contrast agents for both imaging and targeted therapy in a rat xenograft tumor model [20]. HSA-SPIO provided better contrast compared to a control with the TA signal doubling 4 h post injection. The HSA-SPIO was also enwrapped in cell-like alginate-polylysine-alginate microcapsules sensitive to microwaves. Whereas unencapsulated HSA-SPIO were stable for TAI, the encapsulated microcapsules when exposed to short microwave pulses would "pop" and produce a shockwave that destroyed tumor cells. Survival studies guided by TA imaging demonstrated higher survival post treatment with HSA-SPIO compared to control rats by slowing tumor growth in both subcutaneous and deep seated rat tumors [20].

This review described recent progress in ultrasound elastography and hybrid modalities that integrate ultrasound, light and microwaves for early detection and staging of tumors, guiding needle biopsies, and tracking tumor metastasis to the LNs. Each method is safe, noninvasive, and offers unique contrast for characterizing suspicious lesions and the tumor microenvironment in real-time. By combining these techniques with smart contrast agents, new paradigms for

cancer imaging and therapy may emerge in the near future that challenge conventional methods for diagnosing, staging and treating cancer and metastatic disease.

References

1. Barr RG, Destounis S, Lackey LB, Svensson WE, Balleyguier C, Smith C (2012) Evaluation of breast lesions using sonographic elasticity imaging: a multicenter trial. J Ultrasound Med 31(2):281–287
2. Sayed A, Layne G, Abraham J, Mukdadi OM (2014) 3-D visualization and non-linear tissue classification of breast tumors using ultrasound elastography in vivo. Ultrasound Med Biol 40(7):1490–1502
3. Yang Y, Xu X, Guo L, He Y, Wang D, Liu B, Zhao C, Chen B, Xu H (2017) Qualitative and quantitative analysis with a novel shear wave speed imaging for differential diagnosis of breast lesions. Sci Rep 7:40964
4. Leemans CR, Tiwari R, Nauta JJ, van der Waal I, Snow GB (1993) Regional lymph node involvement and its significance in the development of distant metastases in head and neck carcinoma. Cancer 71(2):452–456
5. Ho F, Tham IW, Earnest A, Lee KM, Lu JJ (2012) Patterns of regional lymph node metastasis of nasopharyngeal carcinoma: a meta-analysis of clinical evidence. BMC Cancer 12:98
6. Azizi G, Keller JM, Mayo ML, Piper K, Puett D, Earp KM, Malchoff CD (2016) Shear wave elastography and cervical lymph nodes: predicting malignancy. Ultrasound Med Biol 42(6):1273–1281
7. Chen BB, Li J, Guan Y, Xiao WW, Zhao C, Lu TX, Han F (2018) The value of shear wave elastography in predicting for undiagnosed small cervical lymph node metastasis in nasopharyngeal carcinoma: a preliminary study. Eur J Radiol 103:19–24
8. Ting CE, Yeong CH, Ng KH, Abdulla BJJ, Ting HE (2015) Accuracy of tissue elasticity measurement using shear wave ultrasound elastography: a comparative phantom study. In: World congress on medical physics and biomedical engineering. Springer, Toronto, pp 252–255
9. Menezes GLG, Pijnappel RM, Meeuwis C, Bisschops R, Veltman J, Lavin PT, van de Vijver MJ, Mann RM (2018) Downgrading of breast masses suspicious for cancer by using optoacoustic breast imaging. Radiology 17:170500
10. Lin L, Hu P, Shi J, Appleton CM, Maslov K, Li L, Zhang R, Wang LV (2018) Single-breath-hold photoacoustic computed tomography of the breast. Nat Commun 9(1):2352
11. Garcia-Uribe A, Erpelding TN, Krumholz A, Ke H, Maslov K, Appleton C, Margenthaler JA, Wang LV (2015) Dual-modality photoacoustic and ultrasound imaging system for noninvasive sentinel lymph node detection in patients with breast cancer. Sci Rep 5:15748
12. Forbrich A, Heinmiller A, Zemp RJ (2017) Photoacoustic imaging of lymphatic pumping. J Biomed Opt 22(10):106003
13. Stoffels I, Morscher S, Helfrich I, Hillen U, Leyh J, Burton NC, Sardella TC, Claussen J, Poeppel TD, Bachmann HS, Roesch A, Griewank K, Schadendorf D, Gunzer M, Klode J (2015) Metastatic status of sentinel lymph nodes in melanoma determined noninvasively with multispectral optoacoustic imaging. Sci Transl Med 7(317):317ra199
14. Luke GP, Myers JN, Emelianov SY, Sokolov KV (2014) Sentinel lymph node biopsy revisited: ultrasound-guided photoacoustic detection of micrometastases using molecularly targeted plasmonic nanosensors. Cancer Res 74(19):5397–5408
15. Yang L, Cheng J, Chen Y, Yu S, Liu F, Sun Y, Chen Y, Ran H (2017) Phase-transition nanodroplets for real-time photoacoustic/ultrasound dual-modality imaging and photothermal therapy of sentinel lymph node in breast cancer. Sci Rep 7:45213
16. Kruger RA, Miller KD, Reynolds HE, Kiser WL, Reinecke DR, Kruger GA (2000) Breast cancer in vivo: contrast enhancement with thermoacoustic CT at 434 MHz—feasibility study. Radiology 216(1):279–283
17. Razansky D, Kellnberger S, Ntziachristos V (2010) Near-field radiofrequency thermoacoustic tomography with impulse excitation. Med Phys 37(9):4602–4607
18. Lou C, Yang S, Ji Z, Chen Q, Xing D (2012) Ultrashort microwave-induced thermoacoustic imaging: a breakthrough in excitation efficiency and spatial resolution. Phys Rev Lett 109:218101
19. Ye F, Ji Z, Ding W, Lou C, Yang S, Xing D (2016) Ultrashort microwave-pumped real-time thermoacoustic breast tumor imaging system. IEEE Trans Med Imaging 35(3):839–844
20. Wen L, Yang S, Zhong J, Zhou Q, Xing D (2017) Thermoacoustic imaging and therapy guidance based on ultra short pulsed microwave pumped thermoelastic effect induced with superparamagnetic iron oxide nanoparticles. Theranostics 7(7):1976–1989